Astron. Astrophys. 338, 511–520 (1998)

ASTRONOMY AND ASTROPHYSICS

Seismology of δ Scuti stars in the Praesepe cluster

II. Identification of radial modes and their associated stellar parameters

M.M. Hernández[1⋆], F. Pérez Hernández[1], E. Michel[2], J.A. Belmonte[1], M.J. Goupil[2], and Y. Lebreton[2]

[1] Instituto de Astrofísica de Canarias, E-38200 La Laguna, Tenerife, Spain
[2] DASGAL, URA CNRS 335, Observatoire de Paris, F-92195 Meudon, France

Received 5 January 1998 / Accepted 20 July 1998

Abstract. An analysis based on a comparison between observations and stellar models has been carried out to identify radial modes of oscillations in several multi-periodic δ Scuti stars of the Praesepe cluster (BU, BN, BW and BS Cnc). The assumption that all the stars considered have common parameters, such as metallicity, distance or age, is imposed as a constraint. Even so, there is a large number of possible solutions, partially caused by the rotational effects on the pulsation frequencies and on the stars' positions in the HR diagram, which need to be parameterized. When pairs of radial modes are assumed to be present in every star, only a few similar identifications are found to be possible, corresponding to a metallicity of $Z \sim 0.030$ and an amount of overshooting of $\alpha_{\rm ov} \sim 0.20$. They are associated with a distance modulus of $\sim$6.43 and an age of $\sim$650 Myr. Estimates of mass and rotation rates for each star are also deduced.

Key words: stars: oscillations – δ Scu – open clusters and associations: individual: Praesepe

1. Introduction

Stellar seismology is one of the most powerful tools for improving our understanding of stellar interiors. Cepheids and RR Lyrae variables in the 1970s (Cox 1980, 1987) and pulsating white dwarfs and the Sun in the 1980s and 1990s (Brown & Gilliland 1994) have been the best exploited examples of asteroseismological targets. Apart for the Sun, δ Scuti stars are one of the best non-peculiar main sequence stars for seismological purposes. They are moderate-amplitude pulsators (typically ~ 20 mmag, although larger values can also be found) with pulsation period $P < 0.3$ day, located on or just above the main sequence within the instability strip induced by the κ-mechanism. Most of these A–F stars range from 1.5 to 2.5 $M_\odot$, having a small convective core in their interior. This peculiarity makes δ Scuti stars potentially interesting objects for investigating the overshooting processes at the boundary of convective cores (e.g. Dziembowski & Pamyatnykh 1991).

Several attempts have been made to obtain stellar information from δ Scuti stars (e.g. Mangeney et al. 1991; Goupil et al. 1993; Pérez Hernández et al. 1995; Guzik & Bradley 1995). All have had to face the absence of the greater part of the theoretical modes in the observed spectrum. Noise level, selection mechanisms, geometrical effects and also mutual interference between very close modes (as recently illustrated by Belmonte et al. 1997) contribute towards explaining this phenomenon. Even in the case of a large number of detected modes, such as those found in the field star FG Vir (Breger et al. 1995, 1998), the uncertainties in the stellar parameters prevent a unique identification of the observed frequencies (values of the radial order, n, the degree, l, and the azimuthal order, m, for each frequency peak observed). On the other hand, observational techniques designed to obtain the mode degree (Watson 1988; Garrido et al. 1990; Aerts 1996; Kennelly & Walker 1996; Viskum et al. 1998) have been developed over the last two decades but more work is needed before a systematic application can be carried out. Therefore, at the present stage, to solve the problem of mode identification, situations where additional stellar information can be obtained, such as binary systems and close open clusters, must be considered. Goupil et al. (1993) analysed the star GX Peg, one of the few δ Scuti members of a binary system. In this case, information concerning the inclination angle, i, the rotation rate (assuming synchronization of the system) and the ratio $M_2/(M_2+M_1)$, was employed in the treatment. Moreover, Pérez Hernández et al. (1995) tried to obtain a joint identification for the observed modes in BN and BU Cnc, two δ Scuti stars belonging to Praesepe cluster. The constraints imposed by the cluster parameters proved to be very useful, even though they did not provide a definite mode identification.

Increasing the number of pulsating stars in the same cluster is expected to improve the analysis. For this purpose a very good target is Praesepe, which has the largest known sample of δ Scuti stars in a cluster (14) spread over different evolutionary stages, from the main sequence to the sub-giant phase. Potentially, this would allow scanning for structural changes in the evolution along the main sequence. The international network STEPHI (STellar PHotometry International, Michel et al. 1995) has made a great effort at organizing several three-week three-continent monitoring observations of Praesepe δ Scuti stars in

Send offprint requests to: M.M. Hernández, (mmanuel@iac.es)
⋆ Also Associated Researcher at DASGAL

recent years (see Belmonte et al. 1997 and references therein). Most of the observational frequency data used here come from these network campaigns.

Concerning the mode identification, an attractive but somehow naive strategy would consist in computing for each star all the models scanning the relevant ranges of parameters and, by fitting the theoretical to the observed frequencies, to select the consistent solutions. Here, by a solution is meant the set of stellar parameters that allows the simultaneous modelling of all the stars considered, and that satisfies all the observables, including the frequencies.

In the absence of any independent information on mode identification, the number of possibilities to investigate is huge. Moreover, such a systematic strategy rests strongly on the idea that models and theoretical frequencies are correctly parameterized. If not, then the set of solutions investigated would not necessarily include the real one. This strategy will become more relevant if an external identification, even a partial one, is available.

Here we have restricted the systematic investigation in two ways. First, there are certain reasons for limiting the work to radial modes. Non-radial modes are very sensitive to the structure and to the details of the input physics, mostly because they frequently develop a g-mode character in age ranges such as that estimated for this cluster. This is why they are considered as an asset for δ Scuti seismology. But, at the present stage of mode identification, this is also why we prefer to deal with radial modes: their frequencies are less sensitive to imprecisions in the input physics and its parameterization, depending mainly on global parameters (i.e. mass, radius). Moreover, the independence on the inclination angle, i, of their observed amplitudes and the smaller effect of rotation on their frequencies, which appears only as second-order perturbations, are in favour of our decision.

Dealing with radial modes only is not restrictive enough, but we can use the fact that frequency ratios of radial modes depend very little on the input stellar parameters, such as mass or chemical composition, at least in the ranges of interest for our stars (even if, as we will show, they do depend on rotation to a non-negligible extent). We therefore propose here to investigate the possible solutions on the hypothesis that each star observed presents in its spectrum two or more radial modes. As we will show, this subset of potential identifications contains solutions associated with realistic determinations of the distance, age and chemical composition of the cluster. They are also consistent with growth rate predictions. Of course, these solutions cannot be considered as based on a secure identification of the modes, but rather as coherent solutions under the assumption made. The physical relevance of such an assumption is not easy to establish a priori but may be discussed to some extent in connection with our final results. We shall take this as a simple working hypothesis in order to permit the otherwise huge problem of mode identification in fast-rotating δ Scuti stars to be handled. In fact, as an insight into this issue, certain relaxations of this constraint will also be considered.

In Sect. 2, we describe the main characteristics of the Praesepe cluster and the four δ Scuti stars under study. The modelling, the range of parameters and the calculation of the eigenfrequencies are discussed in Sect. 3. The steps of the method are developed in Sect. 4. Presentation of the results and their discussion are given in Sect. 5. Finally, we present our conclusions in Sect. 6.

2. The Praesepe cluster and the target stars

Praesepe (NGC 2632) is an intermediate age ($\sim$ 500–800 Myr) Population I cluster. Due to its proximity, the observational parameters of Praesepe are better known than those of other, more distant, clusters. The distance used here was $d = 192 \pm 29$ pc, or in terms of distance modulus, $m_V - M_V = 6.42 \pm 0.33$ (Gatewood & Kiewiet de Jonge 1994). Very recent estimations by *HIPPARCOS* (Mermilliod et al. 1997) will be discussed in Sect. 5.1. For the metallicity, we follow Cayrel de Strobel et al. (1992), who find that $0 \lesssim$ [Fe/H] $\lesssim 0.2$, corresponding to $Z = 0.02$–0.03.

Data on visual magnitudes, colours and membership of Praesepe were obtained from the Geneva Photometric System Catalogue (Rufener 1988). In particular, the colour index $B_2 - V_1$ has been used. In Table 1, the values of $m_V$and $B_2 - V_1$ for our target stars are shown. In addition, values of Strömgren $b - y$ colour index from Hauck & Mermilliod (1990) are also given. KW number represents the nomenclature given by Klein-Wassink (1927) to Praesepe members. Spectral types (ST) were obtained from the SIMBAD database in Strasbourg (France).

We note here that although we limit our work to the stars listed in Table 1, there are other δ Scuti stars in Praesepe for which high quality data are available, such as BQ, BT and EP Cnc. These have not been included in the procedure since BQ Cnc is a binary star the position of whose pulsating component is still unknown in the HR diagram, while BT and EP Cnc are evolved stars to which the method detailed in Sect. 4 is more difficult to apply.

In order to compare with theoretical models, a conversion from (m_V, $B_2 - V_1$) to ($M_{\rm bol}$, $T_{\rm eff}$) is required. In the case of $M_{\rm bol}$, the calibration depends on distance, reddening and bolometric correction. Fortunately, for Praesepe, the reddening effect is negligible (Crawford & Barnes 1969). Bolometric corrections have been estimated from the Schmidt-Kaler calibration (1982). In Table 1, it has been listed $T_{\rm eff}$ estimations for our stars from Geneva (Hauck 1984) and Strömgren (Hauck & Künzli 1996) photometry. More recent calibrations with Geneva photometry offer very similar results (Hauck & Künzli 1996). Both calibrations give a precision of ± 150 K (3σ). However, rotational effects in the HR diagram, as explained below, increase the uncertainty in the determination of $T_{\rm eff}$. In Fig. 1, the HR diagram of Praesepe around the turn-off point is represented. Individual stars are represented by circles, in particular the four δ Scuti stars used in this work are indicated by filled circles.

As mentioned before, rotation plays an important role in the determination of the position of the stars in the HR diagram. This effect is produced by the deformation of the stellar surface

Table 1. Observational properties of the target stars. $T_{\rm eff}$ estimations from calibrations of $B_2 - V_1$ and $b - y$ colour indices have also been included (column 8 and 10, respectively). Last two columns give $M_{\rm bol}$ and $T_{\rm eff}$ of the target stars after correcting for rotation (see Fig. 1). In particular, the range of $T_{\rm eff}$ includes the uncertainty in $v \sin i$ and in the photometric calibration (see text).

Star	KW	HD	ST	m_V	$v \sin i$ (km s^{-1})	$B_2 - V_1$	$T_{\rm eff}$ (K)	$b - y$	$T_{\rm eff}$ (K)	$M_{\rm bol}$	$T_{\rm eff}$ (K)
BU Cnc	207	73576	A7V	7.654	205±21	–0.004	8000	0.104	8000	1.115±0.4	8025–8450
BN Cnc	323	73763	A9V	7.801	130±13	0.016	7850	0.130	7750	1.259±0.4	7775–8150
BW Cnc	340	73798	F0V	8.467	170±17	0.063	7500	0.147	7575	2.035±0.4	7475–7850
BS Cnc	154	73450	A9V	8.482	135±14	0.048	7600	0.149	7550	2.096±0.4	7525–7925

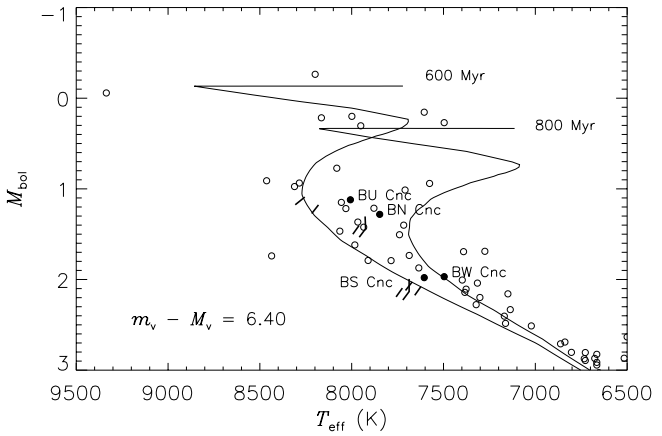

Fig. 1. HR diagram around the turn-off point of the Praesepe cluster. A distance modulus of 6.4 has been considered. Positions of the target stars with (thick lines) and without (filled circles) rotational correction are indicated. The two thick lines for each star represents the corrected positions for the minimum and maximum limit in $v \sin i$ from Table 1. Isochrones corresponding to $Z = 0.03$ and $\alpha_{\rm ov} = 0.20$ and the age indicated in the figure are shown as solid lines.

due to rotation, which introduces changes in the determination of $T_{\rm eff}$ and M_V of the non-rotating copartner that depend on the line-of-sight inclination angle, i, and the projected rotational velocity, $v \sin i$. For our sample of δ Scuti stars, this rotational effect is of the same order as the errors coming from the calibration in $T_{\rm eff}$ or the bolometric correction and will be considered in the analysis. In particular we shall follow the procedure described in Michel et al. (1998) —hereafter Paper I— based on the work by Maeder & Peytremann (1970). Projected rotational velocities, $v \sin i$, were obtained from the SIMBAD database in Strasbourg (France) and are given in Table 1. A 10% uncertainty in this quantity has been assumed. This value follows from taking into account different measurements of $v \sin i$ for a given star, for objects rotating with similar values to ours. In Fig. 1 the positions of the target stars after correcting for this effect are shown as thick lines. Here each star appears to be located in a domain between two lines corresponding to $v \sin i \pm$ quoted error. For a given $v \sin i$, a line is obtained since the correction also depends on i. Limits on i are derived to satisfy a rotation rate between the minimum obtained from $v \sin i$ and the 90% of the break-up rate (see Paper I for more details).

Table 2. Detected frequency peaks in the target stars.

Star		ν (μHz)	Star		ν (μHz)
BU Cnc	ν_1	193.3	BW Cnc	ν_{14}	68.3
	ν_2	195.1		ν_{15}	138.7
	ν_3	200.9		ν_{16}	139.1
	ν_4	215.5		ν_{17}	171.8
	ν_5	228.8		ν_{18}	223.0
	ν_6	229.9		ν_{19}	260.6
	ν_7	276.7		ν_{20}	261.5
				ν_{21}	307.2
BN Cnc	ν_8	263.6		ν_{22}	361.2
	ν_9	266.5			
	ν_{10}	279.5	BS Cnc	ν_{23}	179.7
	ν_{11}	298.1		ν_{24}	197.2
	ν_{12}	300.2		ν_{25}	396.2
	ν_{13}	327.2			

In the last two columns of Table 1, the values of $M_{\rm bol}$ and $T_{\rm eff}$ from Geneva photometry have already been corrected for the rotational effect. The range of values quoted for $M_{\rm bol}$ correspond mainly to the uncertainty in the distance (but, of course, their relative values are more accurately determined) and the range of values considered for $T_{\rm eff}$ has been obtained taking into account the uncertainties in the calibration and in $v \sin i$ (as shown in Fig. 1, the uncertainty in i does not introduce any significant uncertainty in $T_{\rm eff}$ at the level of precision required here). As for $M_{\rm bol}$, relative values of $T_{\rm eff}$ between stars are also better determined. It can be noticed from Table 1, the importance of the rotational correction in $T_{\rm eff}$ compared to the discrepancies in the $T_{\rm eff}$ estimations from the photometrical calibrations.

The frequency peaks detected with a confidence level above 90–99% for our target stars are shown in Table 2. Most of these frequencies come from the STEPHI campaigns as reported by Hernández et al. (1998a) —for more details, see also Belmonte et al. (1994), Álvarez et al. (1998) and Hernández et al. (1998b)—. The frequency resolution in these three-week campaigns is $\Delta\nu \sim 0.5$ μHz. The frequency ν_7 corresponds to a mode detected by Breger et al. (1993) in BU Cnc and is not present later in Belmonte et al. (1994).

3. Stellar models and eigenfrequencies

3.1. Stellar models

Stellar models were calculated using the CESAM stellar evolutionary code (Morel 1997). We considered input physics appropriate to the mass range covered by δ Scuti stars. The nuclear reaction rates are from Caughlan & Fowler (1988). The equation of state is from Eggleton, Faulkner & Flannery (1973). We have used the OPAL radiative opacities (Iglesias, Rogers & Wilson 1992) complemented at low temperatures ($T \leq 10,000$ K) by the Alexander & Ferguson data (1994). The solar mixture of heavy elements from Grevesse (1991) has been chosen, corresponding to the mixture used in opacity calculations. The isotopic ratios are the same as in Maeder (1983). Convection is described according to the classical mixing-length theory (Böhm-Vitense 1958) and the atmosphere is computed using the Eddington $T(\tau)$ law.

With the input physics described above, the solar calibration in luminosity and radius yields an initial solar helium abundance $Y_{\odot} = 0.286$ in mass fraction and a mixing-length parameter $\alpha = l/H_{\rm p} = 1.67$, where $H_{\rm p}$ is the pressure scale-height. The solar mixing-length parameter was used for all the models following investigations of visual binary systems with known masses and metallicity (Fernandes et al. 1998) resulting in similar values of α for a wide range of metallicities and ages. No rotation was included in the calculation of the evolution tracks with CESAM. This is consistent with the corrections made in the colour-magnitude diagram and in the calculation of the eigenfrequencies.

The estimation of the metal content, Z, in Praesepe ranges from 0.02 to 0.03. In order to take a small sampling in metallicity, we have calculated models for $Z = 0.019$, 0.025 and 0.030. Some models take into account an overshooting of the mixed convective core over a distance of $0.20H_{\rm p}$ (i.e. $\alpha_{\rm ov}$= 0.20), following the prescription of Schaller et al. (1992). Recently, Kozhurina-Platais et al. (1997) have suggested a similar value of $\alpha_{\rm ov}$ for another intermediate age open cluster. Models without overshooting have been considered as well. The isochrones corresponding to these models were computed and fitted to the HR diagram of Praesepe, giving distance moduli of 6.15, 6.25 and 6.40 for Z = 0.019, 0.025 and 0.030, respectively. No dependence on overshooting was found. For given model parameters, the distance modulus can be derived with errors no larger than 0.05. In Fig. 1, two isochrones corresponding to $Z = 0.03$ and $\alpha_{\rm ov}= 0.20$ and ages of 600 and 800 Myr are shown. Table 3 summarizes the range of model parameters considered. The age range was chosen according to the isochrones fitted for each value of (Z, $\alpha_{\rm ov}$). This range of ages is wide enough to allow for a correction in $T_{\rm eff}$ and $M_{\rm bol}$ due to rotation. The range of masses considered broadly covers the positions of the target stars, but they are limited to models with hydrogen-core burning within the range of ages estimated. Between 7 and 8 different masses were considered for every set of parameters (Z, $\alpha_{\rm ov}$). From 5 to 15 models covered the range of age, depending on mass.

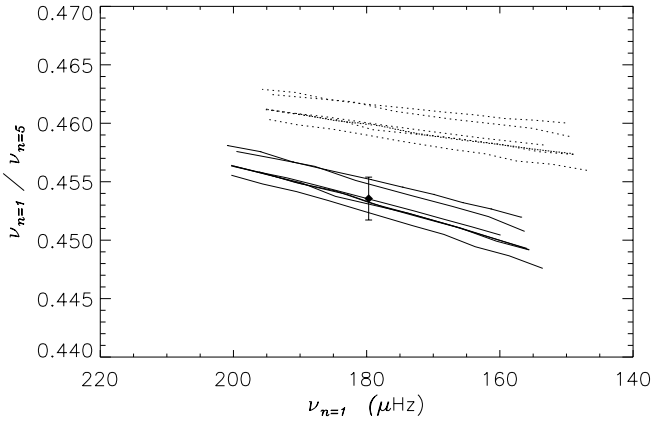

Fig. 2. Frequency ratios of radial modes evolved in a range of ages for $\nu_{\rm rot}$= 0 μHz (solid) and 15 μHz (dotted). Sequences of models for 1.85 $M_{\odot}$ with different metallicity ($Z = 0.019$–0.03), overshooting ($\alpha_{\rm ov}$= 0.00–0.20), helium abundance ($Y = 0.25$–0.29) and mixing length parameter ($\alpha = 1.30$–2.00) have been used. Variations in metallicity produce the largest differences. The filled diamond with error bar corresponds to an observed frequency ratio.

Table 3. Range of model parameters.

Z	$X_{\rm o}$	$\alpha_{\rm ov}$	Mass ($M_{\odot}$)	Age (Myr)
0.019	0.6946	0.00	1.60–2.10	500–700
		0.20	1.60–2.15	600–800
0.025	0.6870	0.00	1.65–2.15	500–700
		0.20	1.65–2.20	600–800
0.030	0.6800	0.00	1.65–2.20	500–700
		0.20	1.65–2.25	600–800

3.2. Radial eigenfrequencies

In order to compute the eigenfrequencies, the models are recalculated using a grid of 1200 points distributed in a suitable way of adequately handling the zones where structural changes are larger, such as the edge of the convective core or the envelope. The theoretical eigenfrequencies have been calculated in the linear and adiabatic approximation as described in Christensen-Dalsgaard & Berthomieu (1991). Richardson's extrapolation was used to improve the solutions.

As mentioned in the introduction, only radial modes ($l = 0$) will be considered. The frequencies of the non-rotating models have been corrected by second-order effects, calculated as in Paper I and based in the work by Saio (1981). A more complete, but computationally expensive, treatment of this effect has been carried out by Soufi et al. (1998). The effect of rotation on the frequencies of the radial modes is a shift to lower frequencies. In particular, the expression of a perturbed frequency, ν'_n, is given by

$$\nu'_n = \nu_n + (Z_n + X) \left(\frac{\nu_{\rm rot}}{\nu_n} \right)^2 , \qquad (1)$$

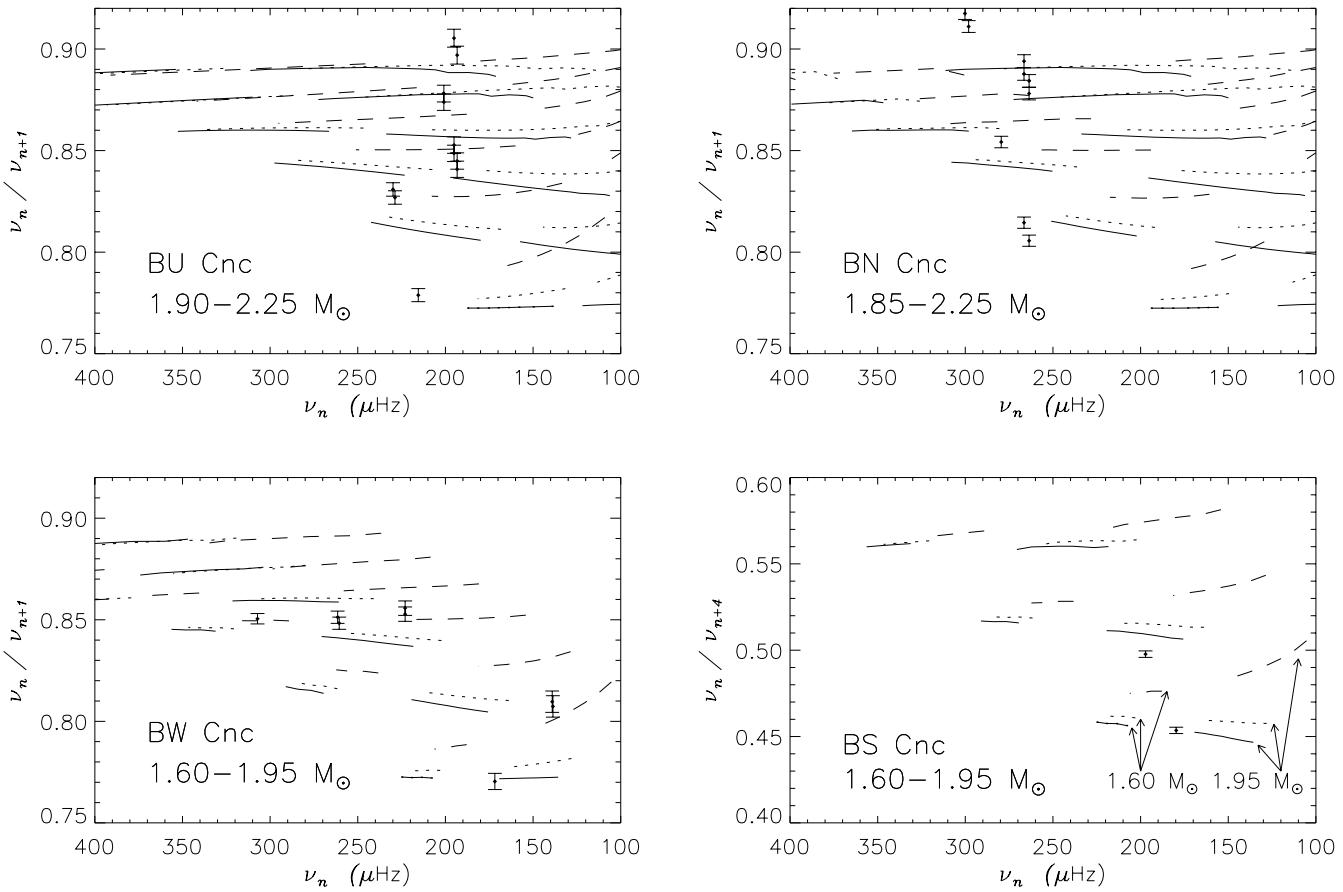

Fig. 3. Theoretical frequency ratios of radial modes for our target stars for $\nu_{\rm rot}$= 0 μHz (solid lines), $\nu_{\rm rot}$= 15 μHz (dotted lines) and $\nu_{\rm rot}$= 30 μHz (dashed lines). Minimum (left) and maximum (right) masses estimated for each star have been evolved in the range of age shown in Table 3. The radial order, n, increases from bottom ($n = 1$) to top. Observational frequency ratios with their error bars are also plotted.

where ν_n is the unperturbed frequency, $\nu_{\rm rot}$ is the rotation rate assumed to be constant throughout the star, and X and Z_n are coefficients that depend on the eigenfunctions.

The value of the rotation rate $\nu_{\rm rot}$ in Eq. 1 needs to be parameterized since the angle of inclination, i, is not known. Its minimum value is given by

$$\nu_{\rm min} = \frac{v \sin i}{2\pi R} \qquad (2)$$

and therefore depends on the stellar radius. Also, for simplicity, we have set the maximum rotation rate to $\nu_{\rm max} = 30$ μHz. Larger $\nu_{\rm rot}$ correspond to rotations very close or larger than the break-up value, depending on the specific model (see Paper I). Given the large values expected for $\nu_{\rm rot}$ for our target stars, the error coming from considering second order terms only can be significant. We shall return to this point in Sect. 4.3.

4. Description of the method

Before describing the whole procedure in detail, we shall illustrate the low sensitivity of the frequency ratios of radial modes to stellar parameters. The largest differences are expected for pair of modes differing substantially in n. In Fig. 2, we have considered the ratio $\nu_{n=1}/\nu_{n=5}$, which for our case is the extreme one. We consider evolution sequences for $M = 1.85\,M_{\odot}$ with different metallicity, overshooting, mixing length parameter and helium abundance (solid lines). Variations in metallicity produce the largest differences. However, none of these model modifications is as important as that induced by rotation. In particular, the dotted lines in Fig. 2 correspond to $\nu_{\rm rot}$= 15 μHz for the same evolutionary sequences as the zero rotation lines. The filled diamond in the figure corresponds to an observed frequency ratio. Here, and in the rest of the paper, the associated errors are calculated from the frequency resolution ($\Delta\nu \sim \pm 0.5$ μHz). For most of the observed frequency peaks, this value represents an overestimate of the actual error, but this has no significant influence on our analysis. From Fig. 2 it follows that although the potential pairs of radial modes present in the observed frequencies can be identified independently of the models used, they are only valid for a specific rotation range.

Basically, the method consists in finding which combinations of potential pairs of radial modes, one per star, give a solution corresponding to models with the same metallicity, overshooting and age while the masses are fixed by a common distance. Observational constraints are applied in order to deter-

mine the initial valid models for every star. With this procedure, we get all the possible identifications of radial modes subject to the constraint of having at least two radial modes in each star. These identifications will be valid only for a restricted range of values for the global parameters of the cluster (Z, $\alpha_{\rm ov}$, d, A).

4.1. Potential pairs of radial modes for each star

For each model considered, we have computed the corresponding frequency ratios between radial modes for different rotation rates. We compare these with the observed ones. In Fig. 3, the most relevant case for each star is shown for $\nu_{\rm rot}$= 0, 15 and 30 μHz. We have computed the ratios for the minimum and maximum masses estimated for each star. For this reason, there are two lines for each radial order and rotation rate. Obviously, any ratio with a frequency ν_n between these two is also valid as a potential identification.

As a first step and for each star, observational frequency ratios are selected as potential pairs of radial modes if they agree with the theoretical ones. 12, 5, 23 and 1 potential pairs of radial modes have been found in BU, BN, BW and BS Cnc, respectively. As mentioned previously, each potential pair will be consistent only for a given range of stellar rotation rates. This must be located between $\nu_{\rm min}$ and $\nu_{\rm max}$ as given in Sect. 3.2. However, since $\nu_{\rm min}$ depends on stellar radius, we shall impose this constraint later.

As a second step, we need to select for each potential ratio the corresponding models with values of ($M_{\rm bol}$, $T_{\rm eff}$) within the observational limits for each star. This is done as follows. For each potential pair of radial modes previously obtained, a given value of n is associated. We compute the corresponding unperturbed frequencies ν_n for a sequence of models with a given (Z, $\alpha_{\rm ov}$). Those models that differ in mass, M, and age, A, can be characterized also by $M_{\rm bol}$ and $T_{\rm eff}$. The theoretical frequencies, ν_n , depend in a simple way on these parameters. An example is given in Fig. 4. Here a spline interpolation in age, A, and mass, M, between the actually computed models has been carried out. The observational constraints in $M_{\rm bol}$ and $T_{\rm eff}$ as given in Table 1 can then be imposed.

However, the observational frequencies must be compared with the perturbed model frequencies, ν'_n. Alternatively, we can subtract the rotational perturbation from the observed frequencies. Since this depends on $\nu_{\rm rot}$ which is determined only within a range from the frequency ratios, there is a corresponding range in ν_n for which the theoretical and the "non rotating" copartner of the observed frequency are expected to agree. Therefore, in Fig. 4, models with $M_{\rm bol}$, $T_{\rm eff}$ and ν_n in the corresponding intervals are selected. This procedure is carried out for different (Z, $\alpha_{\rm ov}$) for each potential ratio. The result is a set of possible models within a range ($M_{\rm bol}$, $T_{\rm eff}$, Z , $\alpha_{\rm ov}$) or, equivalently, (Z, $\alpha_{\rm ov}$, M, A) for each potential pair of radial modes. We note also that a restricted range of $\nu_{\rm rot}$ is obtained.

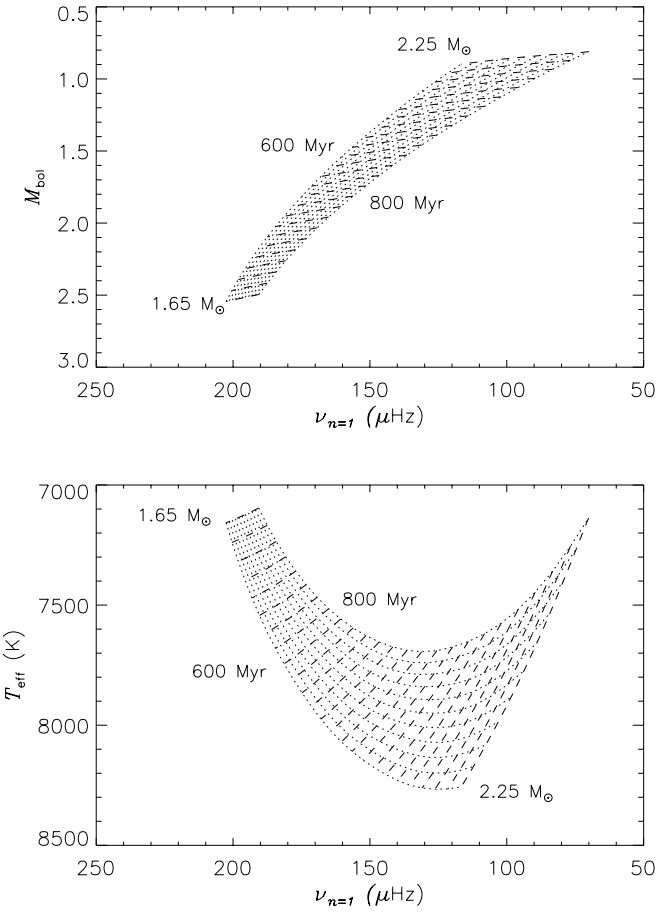

Fig. 4. Representation of $M_{\rm bol}$ and $T_{\rm eff}$ vs. ν_n for models corresponding to the masses and ages shown in Table 3 for ($Z = 0.03$, $\alpha_{\rm ov}$= 0.20) with $n = 1$. Equal mass (dashed) and equal age (dotted) lines are plotted.

4.2. Potential pairs of radial modes coherent with the cluster parameters

The third step is to search for an identification that satisfies the cluster parameters, selecting those solutions with the same age, distance and chemical composition for all the target stars. Assuming that the error in $M_{\rm bol}$ is given mainly by the error in distance, a correspondence can be established between M and d for given A, Z and $\alpha_{\rm ov}$ values. In this way, a domain (Z, $\alpha_{\rm ov}$, d, A) of valid models is obtained for each potential ratio. These parameters must be the same for all the target stars. Thus, we choose one potential ratio per star and check if there is a common domain in (Z, $\alpha_{\rm ov}$, d, A). The same procedure is carried out for all the possible combinations of four potential pairs, one per star.

At this step, we reject those models with $\nu_{\rm rot}$ smaller than $\nu_{\rm min}$ given by Eq. 2. This $\nu_{\rm rot}$ is obtained from Eq. 1 by considering ν'_n as the observed frequency and ν_n as the theoretical frequency for the particular model under consideration.

In this way, we obtain all the possible solutions that contain at least two radial modes per star.

Table 4. Number of possible identifications for each (Z, $\alpha_{\rm ov}$) for different values of ϵ (in μHz).

(Z, $\alpha_{\rm ov}$)	$\epsilon \leq$	0	1	2	3	4	5	10
($Z = 0.019$, $\alpha_{\rm ov} = 0.00$)		0	0	0	0	0	0	0
($Z = 0.019$, $\alpha_{\rm ov} = 0.20$)		0	0	0	0	0	0	0
($Z = 0.025$, $\alpha_{\rm ov} = 0.00$)		0	0	0	0	0	0	0
($Z = 0.025$, $\alpha_{\rm ov} = 0.20$)		0	0	0	0	0	0	63
($Z = 0.030$, $\alpha_{\rm ov} = 0.00$)		0	0	0	0	6	6	121
($Z = 0.030$, $\alpha_{\rm ov} = 0.20$)		0	0	6	9	18	24	142

4.3. Additional uncertainties

We return now to the estimation of the theoretical uncertainties in the frequencies. As previously, this was determined only from the corresponding uncertainty in $\nu_{\rm rot}$. In particular, in the determination of the valid models for each potential pair we considered an interval $[\nu_n - \Delta\nu_n, \nu_n + \Delta\nu_n]$ for the non-rotating copartner frequencies determined from the correction in the rotational perturbation term as given by the maximum and minimum rotation rate. In fact, for large values of $\nu_{\rm rot}$ it is to be expected that this is the dominant term, but when $\nu_{\rm rot}$ is small so is $\Delta\nu_n$. In particular, for BS Cnc one obtains $\Delta\nu_n \leq 1$ μHz. At least in this case, the uncertainty in $\Delta\nu_n$ is comparable with other model uncertainties, such as changes in the opacity tables, hydrogen content and the effect of rotation on the evolution of the stars. In addition, the conversion from the range of rotation rates derived from the frequency ratios to a frequency interval $\Delta\nu_n$ depends slightly on the mass and other parameters of the models. Finally, as commented before, the error in the frequency correction due to the use of Eq. 1 needs to be taken into account. Thus, we have introduced a frequency uncertainty, ϵ, in the estimate of ν_n that is assumed to include all these errors. On one hand, this increases $\Delta\nu_n$ by an amount ϵ; on the other, it increases the range of $\nu_{\rm rot}$ associated with the models.

5. Results and discussion

5.1. Solutions for the four stars

In Table 4, the number of possible identifications, each one with a common domain in (Z, $\alpha_{\rm ov}$, d, A) for the four stars, is shown grouped for each (Z, $\alpha_{\rm ov}$). Different maximum values for ϵ have been considered. For each identification there are a couple of radial frequencies per star. No solution with three radial modes for the same star was found.

Certain features can be derived from these general results:

- Since for a given star some of the observational frequencies are close (see Table 2), they can match at the same theoretical ν_n value with little difference from the $\nu_{\rm rot}$ values. For this reason, the number of valid combinations is very large, but these combinations are frequently associated with similar model parameters.
- There is no valid combination for models with $Z = 0.019$ and $Z = 0.025$ unless very large values for ϵ are allowed.
- For $Z = 0.03$, the solutions with the smallest ϵ are found for models with overshooting.
- The six identifications for ($Z = 0.03$, $\alpha_{\rm ov} = 0.00$) and $\epsilon \leq 4$ μHz are the same as those for ($Z = 0.03$, $\alpha_{\rm ov} = 0.20$) and $\epsilon \leq 2$ μHz.

These six valid combinations for ($Z = 0.03$, $\alpha_{\rm ov} = 0.20$) at the smallest value of ϵ are detailed in Table 5. For BW and BS Cnc there is a unique identification (radial orders n for given observed ν_i). For BU Cnc there are two possible solutions, while for BN Cnc there are three, but two are very similar in the frequencies involved. Note that the distance modulus ($m_V - M_V$) and the age, A, are the same for all the solutions. This is generally the case for given (Z, $\alpha_{\rm ov}$) values. In Paper I, we showed frequency ranges of mode unstability as given by growth rate calculations. All the solutions in Table 5 are consistent with these estimates.

The distance associated with the identifications in Table 5 agrees very well with that derived from the isochrones for the same values of metallicity and overshooting (see Sect. 3.1). This fact is not a direct consequence of having restricted the initial set of models by using the isochrone fit, because the range of age considered was wide enough (200 Myr). In fact, in Sect. 5.2 we shall find a situation where the two distance estimates do not agree.

It is important to note that the range of ages and distances quoted in Table 5 cannot be interpreted as estimates of uncertainties in these quantities because they depend on ϵ. In fact, there is a minimum ϵ for which these ranges go to zero. To obtain reliable errors on age and distance, one would need an independent estimation for the frequency uncertainties in place of our parameter ϵ. There are also systematic errors that do not require an increase in ϵ but rather produce a shift in the resulting values of d and A and the stellar parameters. For instance, errors in M_V due to the bolometric correction could mainly be of this latter type, because we are dealing with close objects in the HR diagram. For the same reason, errors in the rotational correction in this diagram can also have a systematic behaviour.

The new estimate of distance from *HIPPARCOS* observations for Praesepe cluster is $177 \pm^{10.3}_{9.2}$ pc (Mermilliod et al. 1997), which corresponds to a distance modulus of 6.24 ± 0.12. The distance associated with our identifications fits within the 2-σ error. Systematic errors as those mentioned above could explain this disagreement. Moreover, models with intermediate values of Z and $\alpha_{\rm ov}$ could give valid solutions with associated distances closer to that obtained from *HIPPARCOS* (note that our sample is very crude for this level of accuracy).

The stellar and cluster parameters obtained for each solution are constrained by the observed frequencies and the other observational parameters. It is interesting to separate both effects. As mentioned before, all the solutions in Table 5 give very similar parameters. We shall consider solution C_1. Thus, for each star, we have two observational frequencies identified as radial modes with given radial orders. Fig. 5a shows, in an age–distance diagram, contours where one, two, three or the four stars have associated models with common age and distance.

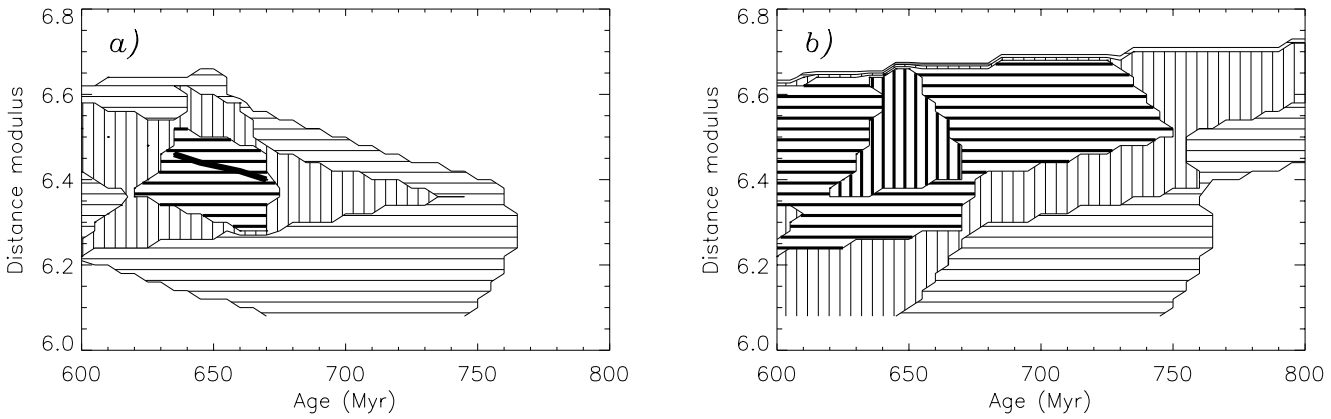

Fig. 5a and b. Distance and age of the valid models common to one (shaded region with horizontal thin lines), two (vertical thin), three (horizontal thick) and four (vertical thick) target stars. **a** Solution C_1 in Table 5 is used. **b** No information from observational frequencies is taken into account.

Table 5. Stellar and global parameters for the six valid combinations with $\epsilon \leq 2$ μHz for $Z = 0.030$ and $\alpha_{\rm ov}$= 0.20. Age, A, is in Myr, mass, M, in $M_{\odot}$ and $\nu_{\rm rot}$ in μHz. ν_i are the observational frequencies given in Table 2.

	$(m_V - M_V)$	A	BU Cnc				BN Cnc				BW Cnc				BS Cnc			
			ν	n	$\nu_{\rm rot}$	M	ν	n	$\nu_{\rm rot}$	M	ν	n	$\nu_{\rm rot}$	M	ν	n	$\nu_{\rm rot}$	M
C_1	6.40–6.46	635–670	ν_3	5	26	2.16	ν_8	5	19	2.10	ν_{19}	3	23	1.82	ν_{23}	1	15	1.80
			ν_5	6			ν_{12}	6			ν_{21}	4			ν_{25}	5		
$C_2 - C_3$	6.40–6.46	635–670	ν_3	5	26	2.16	ν_9	6	25	2.10	ν_{19}	3	23	1.82	ν_{23}	1	15	1.80
			ν_5	6			ν_{11}, ν_{12}	7			ν_{21}	4			ν_{25}	5		
C_4	6.40–6.46	635–670	ν_4	5	23	2.16	ν_8	5	19	2.10	ν_{19}	3	23	1.82	ν_{23}	1	15	1.80
			ν_7	7			ν_{12}	6			ν_{21}	4			ν_{25}	5		
$C_5 - C_6$	6.40–6.46	635–670	ν_4	5	23	2.16	ν_9	6	25	2.10	ν_{19}	3	23	1.82	ν_{23}	1	15	1.80
			ν_7	7			ν_{11}, ν_{12}	7			ν_{21}	4			ν_{25}	5		

This can be compared with Fig. 5b where we have not made use of the observational frequencies (formally it can be thought as taking $\epsilon \rightarrow \infty$). It is clear that the observational frequencies allow us to constrain significantly the possible values for the stellar and cluster parameters provided that any identification in Table 5 is correct.

We can compare the solutions found here with those obtained by Pérez Hernández et al. (1995) for BN and BU Cnc. The two pairs of radial modes proposed in the latter work corresponds to solution C_1. The introduction of the rotational effect in the HR diagram and the smaller $\alpha_{\rm ov}$ used here explain the difference found in age ($\sim$ 650 Myr in the present work and $\sim$ 800 Myr there). The distance modulus obtained here (~ 6.4) is larger than that reported by Pérez Hernández et al. (1995) (~ 6.15). This is probably due to the higher Z required in the present analysis (0.03 rather than 0.025).

5.2. Solutions for three stars: the case of BS Cnc

The analysis carried out in the previous sections is based on the assumption that each star has at least two radial modes of oscillation. Although the results show that there are possible solutions satisfying this hypothesis, we discuss here some relaxation of this assumption by considering that one of the stars has only one radial mode or even none. In our method, this is equivalent to rejecting the frequencies of this star.

A first approach to this problem can be obtained by looking at Fig. 5a. The contour for three stars gives the corresponding ranges of ages and distances. But this is only for solution C_1 in Table 5. In general, after rejecting one star, more solutions than those reported before can be found and some of them can also match at other Z and $\alpha_{\rm ov}$ values. We shall consider these possibilities now.

If BU, BN or BW are not considered, the results are similar to those found previously. In particular, for the smallest ϵ ($\leq$ 2 μHz) the common identifications for the other 3 stars are just those given in Table 5. As might be expected, the number of corresponding models that fit at the same ϵ is larger. For instance, some of the solutions match at $\epsilon \leq 2$ μHz not only for $Z = 0.03$ and $\alpha_{\rm ov}$= 0.20 (as in the solutions for the four stars) but also for models with $Z = 0.03$ without overshooting and for models with $Z = 0.025$, with and without overshooting. However, the models with $Z = 0.025$ give a distance modulus of $(m_V - M_V) \simeq 6.5$–6.6 while the isochrones for this metallicity

give $(m_V - M_V) = 6.25 \pm 0.05$ (see Sect. 3.1). Thus, these solutions must be rejected. For $Z = 0.03$, the range of ages and distances are enlarged respect to those found before: $A = 540$–670 Myr and $(m_V - M_V) = 6.40$–6.50 for $\epsilon \leq 2$ μHz.

If the star not considered is BS Cnc, the situation is different. First, there are solutions for $\epsilon = 0$. This happens because for the remaining stars the uncertainty $\Delta\nu_n$ is larger due to the larger rotational rates estimated for them. This point was commented on in Sect. 4, and shows that if BS Cnc would have two radial modes among those detected, it would impose the strongest constraints. The identifications given in Table 5 still remain valid, but there are more possible solutions. Concerning the stellar parameters, there are solutions for $Z = 0.03$ and $Z = 0.025$ with and without overshooting, while for the solar metallicity no solution is found. The corresponding range of ages is A = 510–750 Myr and the range of distance modulus is $m_V - M_V = 6.2$–6.5. In this case, the distance derived from the observed frequencies and from the isochrones are in agreement for both metallicities. It is also in complete agreement with the distance obtained from *HIPPARCOS*.

6. Conclusions

An attempt has been made to identify radial modes of oscillation in four main sequence δ Scuti stars belonging to Praesepe cluster (BU, BN, BW and BS Cnc) through a comparison between observed and model frequencies.

With the procedure developed here, we get all the possible identifications of radial modes present in each star under the assumption of having at least two radial modes per star. To each solution corresponds not only an identification of radial modes but also a set of stellar and cluster parameters.

Theoretical calculations based on the κ mechanism give a range of potentially excited radial orders that is in agreement with the frequency range observed. However, for the stars considered here, growth rates predict four or five unstable radial modes (see Paper I) while, as we have shown here, there are at most two radial modes of oscillation in each star. Of course, other radial modes can be excited but to small amplitudes and are thus swamped by the noise in the observed signal.

When the four stars are considered to oscillate with two radial modes, the best fit is obtained for six identifications, but since for one of the stars there are two very close frequencies, in practice, there are only four different solutions in terms of stellar and cluster parameters. For two of the stars the identification is unique ($n = 1$ and $n = 5$ in BS Cnc and $n = 3$ and $n = 4$ in BW Cnc) while for the other stars there are two possible solutions in each case, corresponding to a couple of radial orders among $n = 5, 6, 7$. The different solutions correspond to different rotation rates for each star but the associated models are almost the same. These models have a metallicity of $Z = 0.03$ and an overshooting of $\alpha_{\rm ov}$= 0.20. From these, a distance modulus of ∼6.43 and and age of ∼650 Myr are found. Stellar masses and rotation rates for each star are also obtained. Since the four stars are rather close in the HR diagram, the cluster and stellar parameters can be affected by systematic errors but the mode identifications would remain unchanged. The results reported here did not use the determination of distance from *HIPPARCOS*, but they are consistent to within 2σ.

The small ranges of valid parameters obtained here are mostly constrained by one of the stars, BS Cnc. If this star is not considered in the analysis (that is, if this star does not have two radial modes among the observed frequencies), then there are also models without overshooting that fit the observed frequencies. Also, in this case, models with $Z = 0.025$ are in agreement with the observations but models with the solar metallicity are not. The distance range is now $(m_V - M_V) = 6.2$–6.5 in complete agreement with *HIPPARCOS*. However, if the identification for just one of the other stars is wrong, then, the results will be almost the same as for the four stars.

The analysis of the non-radial modes based on these initial results, which is in progress, could provide additional information. In principle we should be able to reject some of the solutions in Table 5 and, if necessary, search for a different subset of mode identifications from those considered here. However, the frequencies of non-radial modes depend more on rotation than those corresponding to radial modes and their number is larger. Hence, with the present observational data and theoretical knowledge, the possibility of finding a definitive, unique mode identification is unlikely and cannot be separated from the determination of stellar parameters. In any case, a first approach to the truth looking for coherent solutions with the actual information is always possible, while awaiting future improvements, such as the application of observational mode identification methods.

Acknowledgements. This work has been supported by the European Union contract ANTENA, under which the continuous collaboration between authors from the two institutions was made possible. This research has made use of the SIMBAD database operated at CDS, Strasbourg (France).

References

Aerts C., 1996, A&A 314, 115
Alexander D.R., Ferguson J.W., 1994, ApJ 437, 879
Álvarez M., Hernández M.M., Michel E. et al., 1998, A&A (in press)
Belmonte J.A., Michel E., Álvarez M. et al., 1994, A&A 283, 121
Belmonte J.A., Hernández M.M., Pérez Hernández F. et al., 1997, in: IAU Symp. 181, Sounding Solar and Stellar Interiors, eds. J. Provost and F.-X. Schmider, Kluwer Academic Publishers, 357
Böhm-Vitense E., 1958, Zeitschr. Astrophys. 46, 108
Breger M., Stich J., Garrido R. et al., 1993, A&A 271, 482
Breger M., Handler G., Nather R.E. et al., 1995, A&A 297, 473
Breger M., Zima W., Handler G. et al., 1998, A&A 331, 271
Brown T.M., Gilliland R.L., 1994, ARA&A 32, 37
Caughlan G.R., Fowler W.A., 1988, Atomic Data and Nuclear Data Tables 40, 283
Cayrel de Strobel G., Hauck B., François P. et al., 1992, A&AS 95, 273
Christensen-Dalsgaard J., Berthomieu G., 1991, in: Solar Interior and Atmosphere, Space Science Series, eds. A.N. Cox, W.C. Livingston and M. Mathews, Univ. Arizona Press, 401
Cox A.N., 1980, ARA&A 18, 15
Cox A.N., 1987, in: IAU Coll. 95, The Second Conference on Faint Blue Stars, eds. A.G. Davis Philip, D.S. Hayes and J.W. Liebert, L. Davis Press, 161

Crawford D.L., Barnes J.V., 1969, AJ 74, 818
Dziembowski W.A., Pamyatnykh A.A., 1991, A&A 248, L11
Eggleton P.P., Faulkner J., Flannery B.P., 1973, A&A 23, 325
Fernandes J., Lebreton Y., Baglin A., Morel P., 1998, A&A (in press)
Garrido R., García-Lobo E., Rodríguez E., 1990, A&A 234, 262
Gatewood G., Kiewiet de Jonge J., 1994, ApJ 428, 166
Goupil M.J., Michel E., Lebreton Y., Baglin A., 1993, A&A 268, 546
Grevesse N., 1991, in: IAU Symp. 145, Evolution of Stars: The Photospheric Abundance Connection, eds. G. Michaud and A. Tutukov, Kluwer Academic Publishers, 63
Guzik J.A., Bradley P.A., 1995, Baltic Astronomy 4, 442
Hauck B., 1984, in: IAU Symp. 111, Calibration of Fundamental Stellar Quantities, eds. D.S. Hayes, L.E. Pasinetti and A.G.D. Philip, D. Reidel Publishing Company, 271
Hauck B., Künzli M., 1996, Baltic Astronomy 5, 303
Hauck B., Mermilliod M., 1990, A&AS 86, 107
Hernández M.M., Belmonte J.A., Michel E. et al., 1998a, in: IAU Symp. 181, Sounding Solar and Stellar Interiors, eds. J. Provost and F.-X. Schmider, poster volume, Observatoire de la Côte d'Azur – Université de Nice, 225
Hernández M.M., Michel E., Belmonte J.A. et al., 1998b, A&A (in press)
Iglesias C.A., Rogers F.J., Wilson B.G., 1992, ApJ 397, 717
Kennelly E.J., Walker G.A.H., 1996, PASP 108, 327
Klein-Wassink W.J., 1927, Publ. Kapteyn Astron. Lab., 41
Kozhurina-Platais V., Demarque P., Platais I., Orosz J.A., Barnes S., 1997, AJ 113, 1045
Maeder A., 1983, A&A 120, 113
Maeder A., Peytremann E., 1970, A&A 7, 120
Mangeney A., Däppen W., Praderie F., Belmonte J.A., 1991, A&A 244, 351
Mermilliod J.C., Turon C., Robichon N., Arenou F., Lebreton Y., 1997, in: Hipparcos Venice '97, ESA SP-402, 643.
Michel E., Chevreton M., Goupil M.J. et al., 1995, in: Proceedings of Fourth SOHO Workshop: Helioseismology, ESA SP-376, 533
Michel E., Hernández M.M., Houdek G. et al., 1998, A&A (submitted)(Paper I)
Morel P., 1997, A&AS 124, 597
Pérez Hernández F., Claret A., Belmonte J.A., 1995, A&A 295, 113
Rufener F., 1988, Catalogue of Stars Measured in the Geneva Observatory Photometric System, 4th edition, Observatoire de Genève, Geneva
Saio H., 1981, ApJ 244, 299
Schaller G., Schaerer D., Meynet G., Maeder A., 1992, A&AS 96, 269
Schmidt-Kaler Th., 1982 in: Landolt-Börnstein New Series VI/2b, Springer-Verlag, 451
Soufi F., Goupil M.J., Dziembowski W.A., 1998, A&A 334, 911
Viskum M., Kjeldsen H., Bedding T.R. et al., 1998, A&A 335, 549
Watson R.D., 1988, Ap&SS 140, 255